

Photocatalytic *Z/E* isomerization unlocking the stereodivergent construction of axially chiral alkene frameworks

Received: 8 January 2024

Accepted: 31 March 2024

Published online: 16 April 2024

Check for updates

Jie Wang^{1,2}, Jun Gu^{1,2}, Jia-Yu Zou¹, Meng-Jie Zhang¹, Rui Shen¹, Zhiwen Ye¹, Ping-Xun Xu¹ & Ying He¹✉

The past century has witnessed a large number of reports on the *Z/E* isomerization of alkenes. However, the vast majority of them are still limited to the isomerization of di- and tri-substituted alkenes. The stereospecific *Z/E* isomerization of tetrasubstituted alkenes remains to be an underdeveloped area, thus lacking in a stereodivergent synthesis of axially chiral alkenes. Herein we report the atroposelective synthesis of tetrasubstituted alkene analogues by asymmetric allylic substitution-isomerization, followed by their *Z/E* isomerization via triplet energy transfer photocatalysis. In this regard, the stereodivergent synthesis of axially chiral *N*-vinylquinolinones is achieved efficiently. Mechanistic studies indicate that the benzylic radical generation and distribution are two key factors for preserving the enantioselectivities of axially chiral compounds.

Alkenes are fundamental building blocks since their various applications in medicinal and material chemistry, and as chemical platforms in the field of organic synthesis¹. In this context, stereoselective synthesis of alkenes in both *Z*- and *E*-configurations presents a big challenge in organic synthesis^{2–5}. An elegant method to achieve this goal is alkene *Z/E* isomerization which relies upon the unique properties of the C=C bond. Indeed, the *Z/E* isomerization of alkenes can be traced back to 1923 by Herzig and Faltis⁶. After that, synthetic strategies of this transformation is improving by leaps and bounds, including photocatalysis, acid (or base) catalysis, and metal catalysis^{7–13}. Despite these advances, the *Z/E* isomerization are mainly limited to the di- and tri-substituted alkenes (Fig. 1A). In contrast, the isomerization of tetrasubstituted alkenes is more challenging and less reported (Fig. 1B)^{14–16}. The pioneering work in this area was the reports on molecular motors by Nobel laureate B. Feringa^{17–21}. In this regard, the photoinduced *cis-trans* isomerizations of helical alkenes with a 180° rotation around the C=C bond were established. The molecular motor would undergo 360° rotation by combining the photochemical and thermal isomerization. Herein the point chiral elements that existed in the molecular motor are one of the essential factors for this tetrasubstituted alkene isomerization. In 2020, another seminal work on *Z/E* isomerization of

boron-containing tetrasubstituted alkenes by photocatalysis was reported. A subtle 90° C(sp²)-B bond rotation intermediate was proposed to achieve the directional *E* to *Z* isomerization¹⁴. Nonetheless, the stereospecific *Z/E* isomerization of acyclic axially chiral alkene analogs remains elusive (Fig. 1B).

Axially chiral alkenes was first mentioned and proposed by Kawabata in 1991 during the research on the memory of chirality²². It is only in recent years that studies for their catalytic synthesis were initiated^{23–25}. Accordingly, several typical synthetic methods have been developed to date^{26–33}. Among these, asymmetric allylic substitution-isomerization (*AASI*) which was developed by our group, has emerged as an appealing strategy for the synthesis of axially chiral alkene analogs^{34–38}. Unlike other strategies relying on very complex specific substrates, *AASI* can provide a versatile and modular way to accomplish the construction by using easily accessible allylic carbonate electrophiles and sterically bulky nucleophiles. Inspired by *AASI* and alkene *Z/E* isomerization, we envision that the stereodivergent synthesis of axially chiral tetrasubstituted alkenes could be achieved by combining *AASI* with geometrical *Z/E* isomerization. Ideally, such axially chiral *Z* (or *E*) alkene could be isomerized to its corresponding *E* (or *Z*) configuration while maintaining the enantioselectivity.

¹School of Chemistry and Chemical Engineering, Nanjing University of Science and Technology, Nanjing 210094, China. ²These authors contributed equally: Jie Wang, Jun Gu. ✉e-mail: yhe@njust.edu.cn

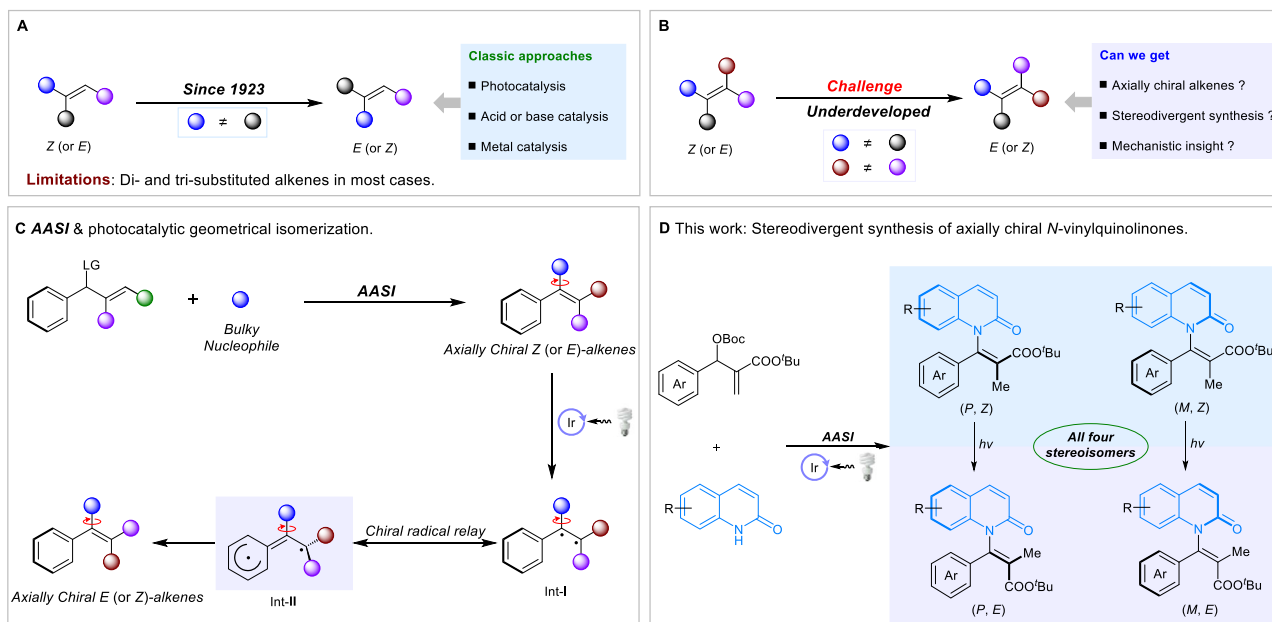


Fig. 1 | State of the art for the stereodivergent synthesis of axially chiral alkene analogs. A Z/E isomerization of di- and tri-substituted alkenes. **B** Z/E isomerization of tetrasubstituted alkenes. **C** Asymmetric allylic substitution-isomerization and

photocatalytic geometrical Z/E isomerization. **D** Stereodivergent synthesis of axially chiral N -vinylquinolinones.

To this end, we posit that the Z axially chiral styrene analogs, which are synthesized by AASI herein, could isomerize to their corresponding E products by a photocatalytic isomerization. As shown in Fig. 1C, the ground-state alkenes could be excited to a higher energy triplet state radical by energy transfer (EnT) process^{39–43}, thus leading to the intermediate **I**. The phenyl ring would distribute the benzyl radical with the chiral radical relay^{44,45}, which affords the transient axially chiral intermediate **II**. Afterward, the bond rotation occurs while preserving the axial chirality around the C–N axes. At last, the radical recombination would give the corresponding E axially chiral styrene analogs. However, in our own assessment, there are still several challenges that are addressed to achieve our goal: (1) as for the AASI process, the nucleophiles are sterically bulky that may cause the low reactivity of reaction. In addition, the products must be obtained with high enantioselectivity, regioselectivity and geometrical (Z/E) selectivity simultaneously; (2) as for the photocatalytic isomerization process, the initial excitation via energy transfer creates a triplet biradical that may permit free rotation around the chiral axis, thus leading to the loss of axially chiral information.

Herein, we report the atroposelective synthesis of axially chiral N -vinylquinolinones by AASI and photocatalytic geometrical Z/E isomerization that leads to the stereodivergent synthesis of tetrasubstituted alkenes (Fig. 1D).

Results and discussion

We commenced our studies by investigating the chiral Lewis base-catalyzed asymmetric allylic substitution (AAS) of Morita–Baylis–Hillman (MBH) esters **1a** with 2(1H)-quinolinone **2a**. The reaction optimization revealed that the enantioenriched β -substituted allylic intermediate (**Int-3a**) was first generated in high yield and enantioselectivity when using (DHQD)₂PYR as the catalyst. Afterward, the use of inorganic base MeONa promoted the isomerization effectively that afforded axially chiral product **3a** in high yield and enantiospecificity (es) with Z/E ratio beyond 19/1 (see Supplementary Fig. 2). It should be noted that the two-step processes could be carried out in one-pot which gave the product (P,Z)-**3a** in 87% yield and 94% enantiomeric excess (ee) (Fig. 2). With the optimized conditions in hand, we then explored the scope of the reaction. Pleasingly, a wide range of aryl

MBH esters bearing *para*- and *meta*-substituents were accommodated, affording (P,Z)-(**3b–3j**) in 74–92% yield with 88–95% ee. Furthermore, a number of fused-rings and heterocycles were well-tolerated, including a naphthalene [(P,Z)-**3k**], a thiophene [(P,Z)-**3l**] and a benzothiophene [(P,Z)-**3m**]. With respect to the 2(1H)-quinolinone scope, various substituents at different sites on quinolinone ring were then studied (Fig. 2). The reaction of 2(1H)-quinolinones bearing electron-donating and electron-withdrawing groups at the C4 position proceeded smoothly, affording products (P,Z)-(**3n–3r**) in 65–79% yield with 92–96% ee. Moreover, substituents attached at the C5, C6 or C7 sites were all compatible with the reaction conditions, affording axially chiral N -vinylquinolinones (P,Z)-(**3s–3x**) in 56–84% yields with 93–97% ee. The high compatibility of the reaction system encouraged us to investigate its practicality for late-stage functionalization. In this context, substrates derived from *L*-menthol and vitamin E underwent the AASI smoothly, giving the products (P,Z)-**3y** and (P,Z)-**3z** in 72% and 64% yield with >20/1 diastereomeric ratio (dr), respectively. These results offer a general and promising approach for the functionalization of late-stage molecules to axially chiral compounds. Of note, in all cases, axially chiral N -vinylquinolinones **3** were obtained in high Z -selectivities. The absolute configuration of (P,Z)-**3a** and (P,Z)-**3m** were confirmed by single-crystal X-ray analysis, and others were assigned by analogy.

Having established the strategy for the synthesis of **3** in Z configuration, we investigated the feasibility of photocatalytic geometrical Z/E isomerization of (P,Z)-**3** to (P,E)-**3**. If successful, it would represent a rare example of accessing axially chiral styrene analogs in both E and Z stereoisomers, thus providing the possibility for the stereodivergent synthesis of alkenes. As shown in Table 1, we were pleased to find that (P,Z)-**3a** could isomerize to (P,E)-**3a** in the presence of photosensitizer *fac*-Ir(ppy)₃ ($E_T = 58.1 \text{ kcal mol}^{-1}$) under the irradiation of 420 nm light-emitting diodes (LED)^{46,47}. Although only moderate E/Z ratio was observed, (P,E)-**3a** was efficiently afforded in 93% ee (99% es). The absolute configuration of (P,E)-**3a** were unambiguously determined by single-crystal X-ray analysis. This result revealed the high efficiency of the geometric Z/E isomerization of tetrasubstituted alkene. Other photosensitizers such as Ru(bpy)₃Cl₂·6H₂O and 2,3,5,6-tetrakis(carbazol-9-yl)-1,4-dicyanobenzene (4CzTPN) was proved to be

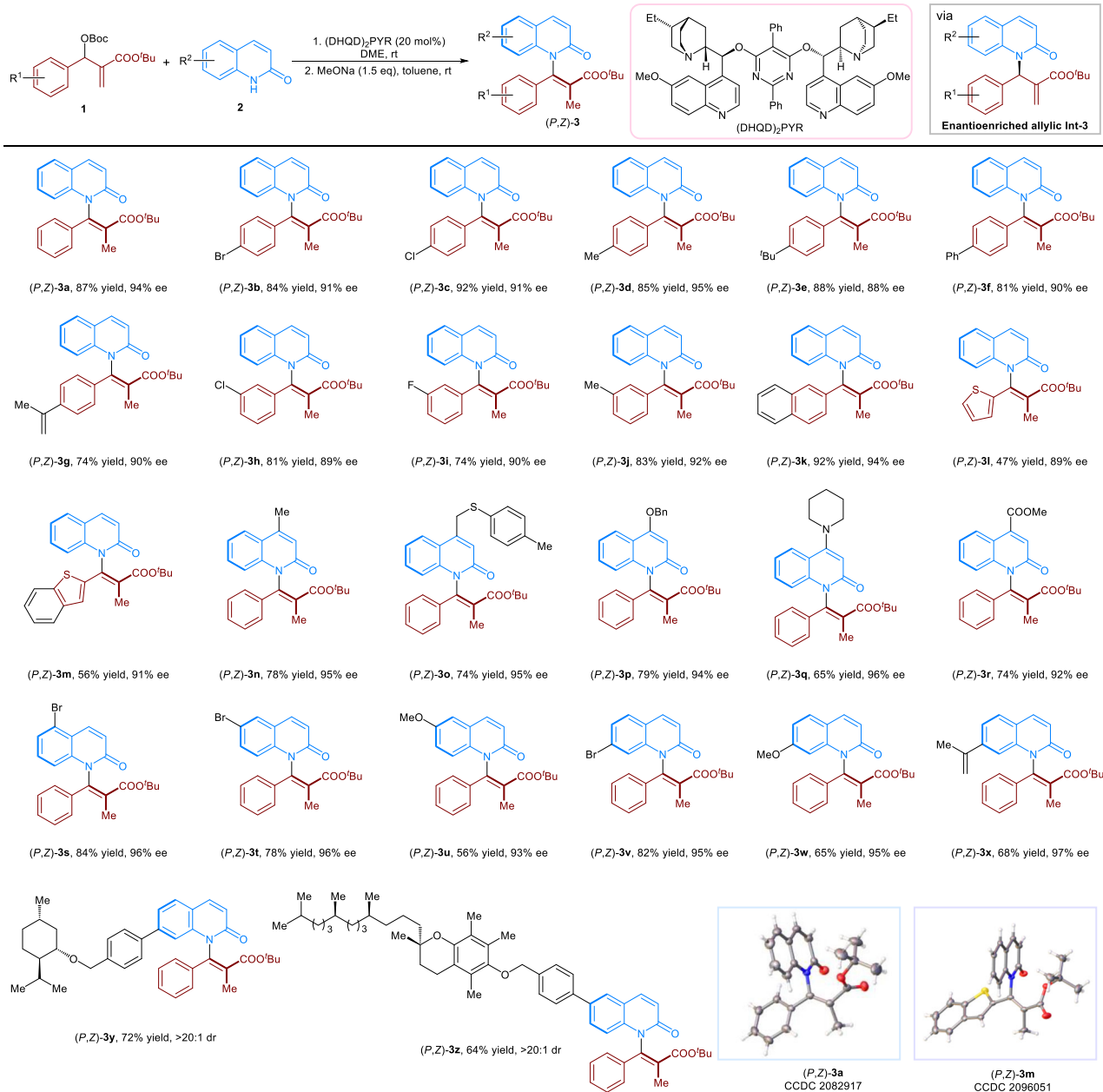


Fig. 2 | Substrate scope of AASI. Reaction conditions, **1** (0.9 mmol), **2** (0.3 mmol), (DHQD)₂PYPYR (20 mol%), 1,2-dimethoxyethane (DME) (1.5 mL), rt for 48 h. NaOMe (0.45 mmol), and toluene (1.0 mL) was then added after the rotary evaporation of

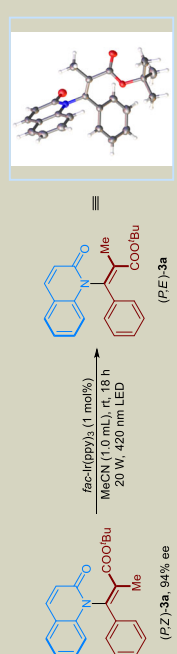
DME. Isolated yield, the ee values were calculated by chiral HPLC traces. The dr ratios were determined by crude ¹H-NMR. The *Z/E* ratios of the products were obtained beyond 19/1.

ineffective (Table 1, entries 2 and 3). The use of {Ir(dtbpy)[dF(CF₃)ppyl]₂PF₆ gave us a moderate *E/Z* ratio with 98% es (entry 4). The examination of the solvent effect suggested that tetrahydrofuran (THF) is the best choice for enhancing the selectivity (*E/Z* = 8/1) (entries 5–7). In this case, (*P,E*)-**3a** was readily isolated in 94% ee (100% es). In addition, no *Z/E* isomerization occurred in the absence of light or photosensitizer (entry 8). To rule out the thermal background reactivity, the reaction was carried out in THF at 60 °C in the absence of the photosensitizer. As a result, no product of (*P,E*)-**3a** was observed (entry 9).

We then investigated the substrate scope of photochemical *Z/E* isomerization. As shown in Fig. 3, the reactions proceeded smoothly when using (*P,Z*)-**3** possessing phenyl moiety with *para*- and *meta*-substituents. In this regard, (*P,E*)-(**3b–3j**) were obtained in 64–86% isolated yields and 99–100% es with *E/Z* ratio up to 15/1. The reaction

also tolerated substrates bearing the fused and heterocyclic ring, affording (*P,E*)-(**3k–3m**) in good yields and enantiospecificities with moderate to good *E/Z* ratios. Different substituents attached at the C4, C5, or C6 sites of the quinolinone ring were also examined. As a result, (*P,E*)-(**3n–3v**) were afforded good to excellent yields and *E/Z* ratios with high es except (*P,E*)-**3r**. We speculated that the low enantioselectivity of (*P,E*)-**3r** is attributed to the undesired radical fragmentation via the quinolinone ring rather than the phenyl ring. In addition, (*P,Z*)-**3w** were accommodated to the reaction conditions which afforded (*P,E*)-**3w** in excellent yield, ee and *E/Z* ratio. However, the reaction was less reactive when using substrate bearing bulky group at C7 site of the quinolinone ring [(*P,E*)-**3x**]. Of particular note, in all cases, the (*P,Z*)-**3** in the reaction system were recovered without any loss in their enantioselectivities. In addition, the late-stage molecules were also compatible to give (*P,E*)-**3y** and (*P,E*)-**3z** in moderate yields and beyond 20/1 dr.

Table 1 | Optimization of photochemical Z/E isomerization



Entry	Variation from "standard conditions"	E/Z	ee (%)	es (%)
1	None	1/1	93	99
2	Ru(bpy) ₃ Cl ₂ · 6H ₂ O as the photosensitizer	-	-	-
3	4CzTPN as the photosensitizer	-	-	-
4	{Ir(dtbbpy)[dF(CF ₃)ppy] ₂ PF ₆ as the photosensitizer	3/1	92	98
5	Toluene as the solvent	1/1	93	99
6	MeOH as the solvent	3/1	94	100
7	THF as the solvent	8/1	94	100
8	No light or no photosensitizer	-	-	-
9	No photosensitizer, 60 °C in THF	-	-	-

Reaction conditions, (P,Z)-3a (0.1 mmol), photosensitizer (1 mol%), solvent (1.0 mL), rt for 18 h. The ee values of (P,E)-3a were calculated by chiral HPLC traces. The E/Z ratio of 3a was calculated by crude ¹H-NMR after the reactions. Es (enantiospecificity) = [ee_{(P,Z)-3a}]/100%.

With the synthetic advances of our strategy demonstrated, we moved forward to gain insights into photocatalytic Z/E isomerization of (P,Z)-3a. As shown in Fig. 4A, a triplet EnT photocatalytic mechanism was proposed. Photosensitization of (P,Z)-3a by the excited states Ir(ppy)₃ generates the activated diradical intermediate **I**. The rapid benzyl radical distribution occurs to resonate with the key intermediate **II**. In this regard, the high efficiency of enantiospecificity could be anticipated since **II** is still axially chiral intermediates around the C-N axis. The C-C bond of intermediate **II** would be twisted by 90°, which isomerized to the chiral intermediate **III**. The radical redistribution of **III** resonated with the intermediate **IV** would undergo the spin crossover to intermediate **V**, followed by the radical recombination to furnish the product (P,E)-3a.

We subsequently carried out the time-dependent density functional theory (TDDFT) calculations to study the reaction mechanism^{9,46–50}. As shown in Fig. 4B, compared to the energy of (P,Z)-3a, (P,E)-3a is 3.4 kcal/mol lower than (P,Z)-3a. The vertical excitation energies (S₀ → T₁) for (P,Z)-3a and (P,E)-3a were calculated to be 54.5 and 55.9 kcal/mol, respectively, indicating that (P,Z)-3a was more easily activated by the triplet EnT than that of (P,E)-3a. The chiral intermediate **III** would be generated by EnT photocatalysis with the energy of 41.7 kcal/mol (See Supplementary Fig. 6). Due to the axially chiral character of intermediate **III**, in this case, (P,E)-3a was afforded with high enantiospecificity during the isomerization process.

Encouraged by the aforementioned results, we then investigated the stereodivergent synthesis of axially chiral N-vinylquinolinones **3**. To our delight, besides the generation of (P,Z)-3a and (P,Z)-3s (Fig. 5, a), the one-pot synthesis of (P,E)-3a and (P,E)-3s were evaluated which shown the competitive yields and ee (Fig. 5, b). By using (DHQ)₂PYR as the catalyst under similar reaction conditions, (M,Z)-3a and (M,Z)-3s were obtained in both 78% yields with 86% and 88% ee, respectively (Fig. 5, c). Combining AASI and photocatalytic isomerization, (M,E)-3a and (M,E)-3s were readily afforded in 65% yield with 84% ee and 61% yield with 88% ee, respectively (Fig. 5, d).

Considering the potential application of atropisomers in pharmaceutical chemistry^{51,52}, the stereodivergent transformations of axially chiral N-vinylquinolinones **3a** and **3v** were performed (Fig. 6A). First, reduction of **3a** gave all four stereoisomers (P,Z)-4, (M,Z)-4, (P,E)-4 and (M,E)-4 in moderate to good yields while maintaining the corresponding enantioselectivities. In addition, the double addition of **3a** with methylmetallic reagents afforded compounds **5** in all four configurations with high enantiospecificities, from which (P,Z)-5 was unambiguously confirmed by its single-crystal X-ray analysis. On the other hand, the Sonogashira coupling of axially chiral N-vinylquinolinones **3v** with phenylacetylene generated the (P,Z)-6 and (P,E)-6 in excellent yields and enantioselectivities (Fig. 6B). In addition, compounds **3v** could be well-tolerated to the sequential Sonogashira coupling and base-promoted deprotection which gave the (P,Z)-7 and (P,E)-7 in 86% and 93% ee, respectively.

At last, we performed the racemization experiments of axially chiral N-vinylquinolinones **3**. As shown in Fig. 7, comparison of rotational barriers around the C-N axis (Z-3a vs E-3a) indicated that the E-3a (27.0 kcal/mol) has a higher configurational stability than Z-3a (25.7 kcal/mol). These results indicate that the steric hindrance of the tetrahedral methyl group may be bigger than that of the ester group. Although the configurational stability of **3** is not very high, the easy transformation of the ester group in **3** would give axially chiral products in high configurational stabilities. For example, as shown in Fig. 6A, the rotational barriers of Z-4 and Z-5 in toluene are 31.3 and 33.5 kcal/mol, respectively.

In conclusion, we have disclosed the highly efficient photocatalytic Z/E geometrical isomerization of axially chiral alkene analogs. Although alkene geometrical Z/E isomerization has been realized for one century, the stereodivergent synthesis through AASI and photocatalytic Z/E isomerization for accessing tetrasubstituted alkenes

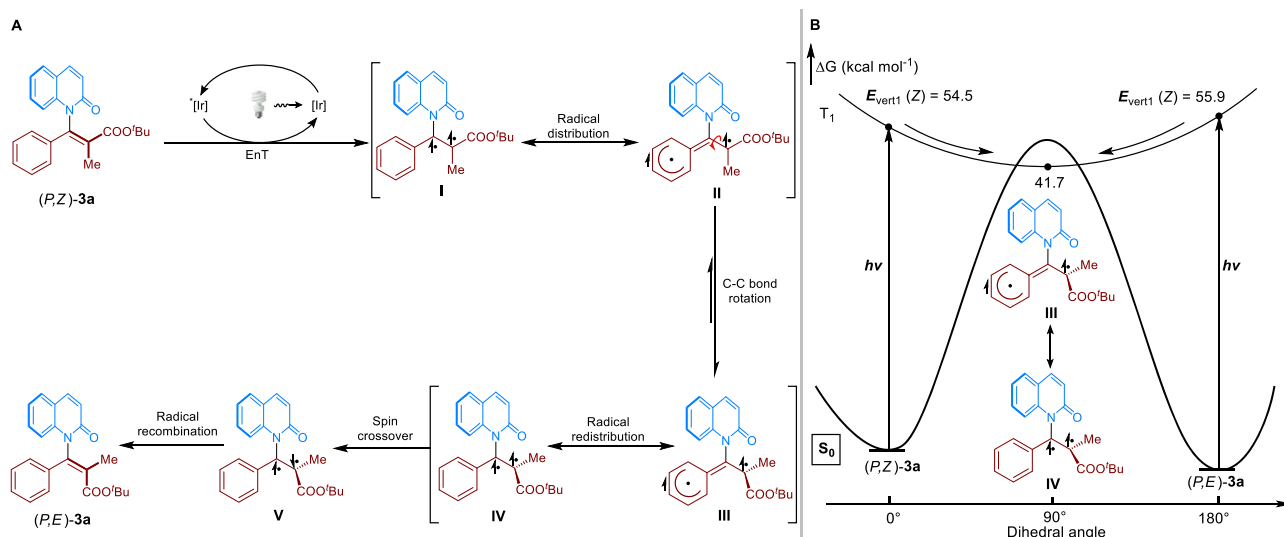


Fig. 4 | Mechanistic studies. **A** Proposed mechanism of *Z/E* isomerization of **3a**. **B** TDDFT studies of *Z/E* isomerization of **3a**. The Gibbs free energy (in kcal/mol) profiles for the photocatalytic *Z/E* isomerization and the optimized structures of

critical intermediates. All energies were calculated at the M06-2X/def2-TZVPP(SMD)//M06-2X/def2-SVP(SMD).

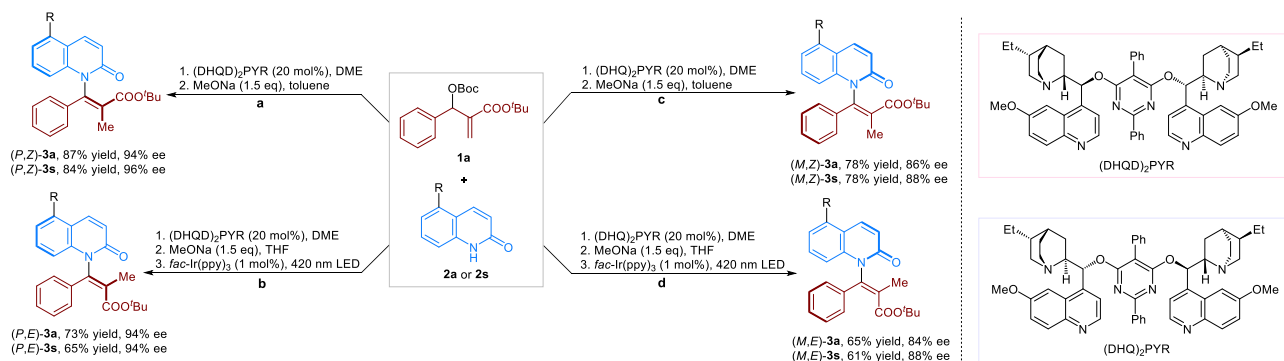


Fig. 5 | Stereodivergent synthesis. Stereodivergent synthesis of axially chiral *N*-vinylquinolones **3a** and **3s**.

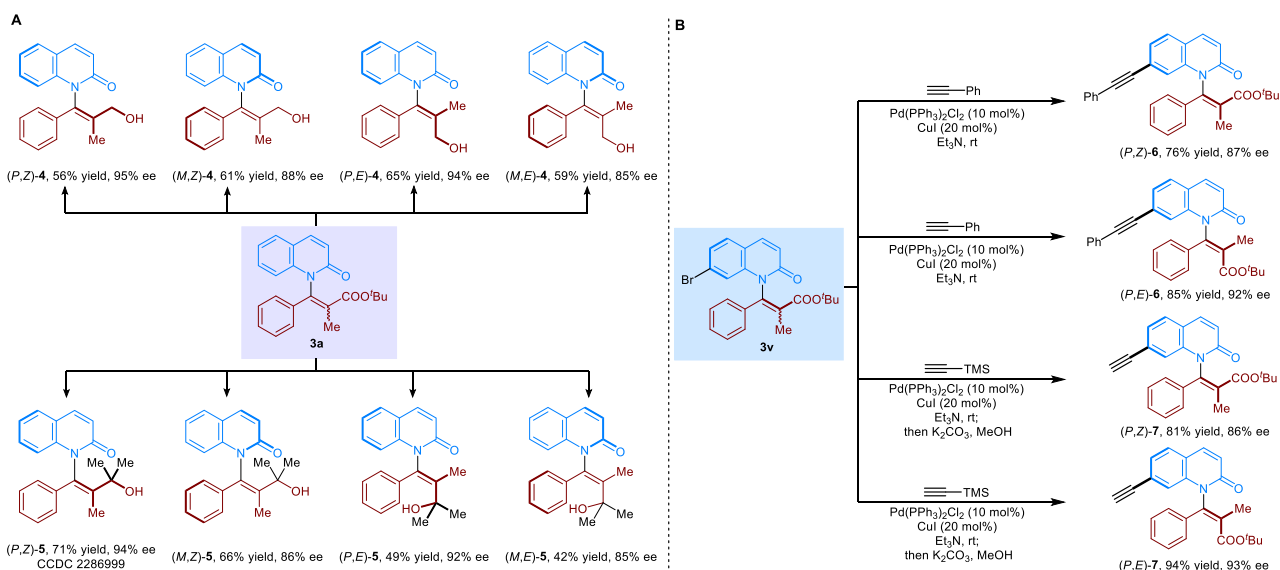


Fig. 6 | Product transformations. **A** Stereodivergent transformations of axially chiral *N*-vinylquinolones **3a**. **B** Stereodivergent transformations of axially chiral *N*-vinylquinolones **3v**.

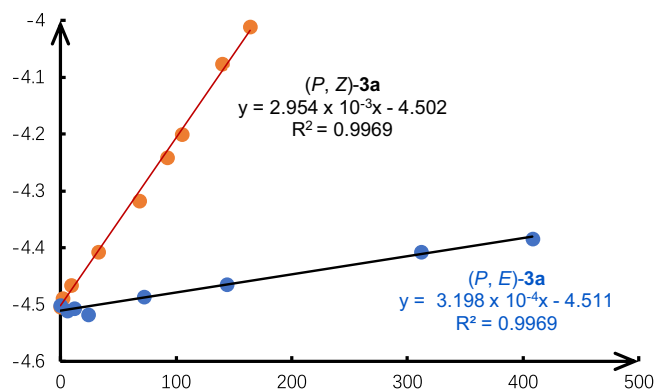


Fig. 7 | Configurational stability studies. Racemization experiments of axially chiral *N*-vinylquinolinones *Z*-**3a** and *E*-**3a**.

chromatography over silica gel (petroleum ether: ethyl acetate = 50:1 to 10:1) to afford the desired product (*P,E*)-**3**. The *Z/E* ratio was determined by crude ¹H-NMR of the reaction mixture.

Data availability

Crystallographic data for the structures reported in this article have been deposited at the Cambridge Crystallographic Data Centre (CCDC), under deposition numbers CCDC 2082917 [(*P,Z*)-**3a**], 2096051 [(*P,Z*)-**3m**], 2089101 (**Int-3a**), 2252177 [(*P,E*)-**3a**] and 2286999 [(*P,Z*)-**5**]. These data can be obtained free of charge from The Cambridge Crystallographic Data Centre via www.ccdc.cam.ac.uk/data_request/cif. Experimental procedures, characterization of new compounds, and all other data supporting the findings are available in the Supplementary Information. All data were available from the corresponding author upon request. Source data are provided with this paper.

References

- Davarnejad, R. (ed). *Alkenes: Recent Advances, New Perspectives and Applications* (IntechOpen, 2021).
- Flynn, A. B. & Ogilvie, W. W. Stereocontrolled synthesis of tetra-substituted olefins. *Chem. Rev.* **107**, 4698–4745 (2007).
- Buttard, F., Sharma, J. & Champagne, P. A. Recent advances in the stereoselective synthesis of acyclic all-carbon tetrasubstituted alkenes. *Chem. Commun.* **57**, 4071–4088 (2021).
- Nguyen, T. T., Koh, M. J., Mann, T. J., Schrock, R. R. & Hoveyda, A. H. Synthesis of *E*- and *Z*-trisubstituted alkenes by catalytic cross-metathesis. *Nature* **552**, 347–354 (2017).
- Zell, D. et al. Stereoconvergent and -divergent synthesis of tetra-substituted alkenes by nickel-catalyzed cross-couplings. *J. Am. Chem. Soc.* **143**, 19078–19090 (2021).
- Herzig, J. & Faltis, F. Zur kenntnis des bixins. *Justus Liebigs Ann. Chem.* **431**, 741–756 (1923).
- Neveselý, T., Wienhold, M., Molloy, J. J. & Gilmour, R. Advances in the *E* → *Z* isomerization of alkenes using small molecule photo-catalysts. *Chem. Rev.* **122**, 2650–2694 (2022).
- Corpas, J., Mauleón, P., Arrayás, R. G. & Carretero, J. C. E. /*Z* photoisomerization of olefins as an emergent strategy for the control of stereodivergence in catalysis. *Adv. Synth. Catal.* **364**, 1348–1370 (2022).
- Huang, M., Zhang, L., Pan, T. & Luo, S. Deracemization through photochemical *E/Z* isomerization of enamines. *Science* **375**, 869–874 (2022).
- Metternich, J. B. & Gilmour, R. A bio-inspired, catalytic *E* → *Z* isomerization of activated olefins. *J. Am. Chem. Soc.* **137**, 11254–11257 (2015).
- Singh, K., Staig, S. J. & Weaver, J. D. Facile synthesis of *Z*-alkenes via uphill catalysis. *J. Am. Chem. Soc.* **136**, 5275–5278 (2014).
- Hao, T. et al. Trace mild acid-catalysed *Z* → *E* isomerization of norbornene-fused stilbene derivatives: intelligent chiral molecular photoswitches with controllable self-recovery. *Chem. Sci.* **12**, 2614–2622 (2021).
- Kudo, E., Sasaki, K., Kawamata, S., Yamamoto, K. & Murahashi, T. Selective *E* to *Z* isomerization of 1,3-dienes enabled by a dinuclear mechanism. *Nat. Commun.* **12**, 1473 (2021).
- Molloy, J. J. et al. Boron-enabled geometric isomerization of alkenes via selective energy-transfer catalysis. *Science* **369**, 302–306 (2020).
- Wienhold, M. et al. Geometric isomerisation of bifunctional alkenyl fluoride linchpins: Stereodivergence in amide and polyene biosostere synthesis. *Angew. Chem. Int. Ed.* **62**, e202304150 (2023).
- Neveselý, T. et al. Leveraging the *n*→*π** interaction in alkene isomerization by selective energy transfer catalysis. *Angew. Chem. Int. Ed.* **61**, e202113600 (2022).
- Koumura, N., Zijlstra, R. W. J., van Delden, R. A., Harada, N. & Feringa, B. L. Light-driven monodirectional molecular rotor. *Nature* **401**, 152–155 (1999).
- Wang, J. & Feringa, B. L. Dynamic control of chiral space in a catalytic asymmetric reaction using a molecular motor. *Science* **331**, 1429–1432 (2011).
- Štacko, P. et al. Locked synchronous rotor motion in a molecular motor. *Science* **356**, 964–968 (2017).
- Kistemaker, J. C. M., Štacko, P., Visser, J. & Feringa, B. L. Unidirectional rotary motion in achiral molecular motors. *Nat. Chem.* **7**, 890–896 (2015).
- Kudernac, T. et al. Electrically driven directional motion of a four-wheeled molecule on a metal surface. *Nature* **479**, 208–211 (2011).
- Kawabata, T., Yahiro, K. & Fujii, K. Memory of chirality: enantioselective alkylation reactions at an asymmetric carbon adjacent to a carbonyl group. *J. Am. Chem. Soc.* **113**, 9694–9696 (1991).
- Feng, J. & Gu, Z. Atropisomerism in styrene: synthesis, stability, and applications. *Synopen* **5**, 68–85 (2021).
- Wu, S., Xiang, S.-H., Cheng, J. K. & Tan, B. Axially chiral alkenes: atroposelective synthesis and applications. *Tetrahedron Chem.* **1**, 100009 (2022).
- Qian, P.-F., Zhou, T. & Shi, B.-F. Transition-metal-catalyzed atroposelective synthesis of axially chiral styrenes. *Chem. Commun.* **59**, 12669–12684 (2023).
- Zheng, S.-C. et al. Organocatalytic atroposelective synthesis of axiallychiral styrenes. *Nat. Commun.* **8**, 15238 (2017).
- Jia, S. et al. Organocatalytic enantioselective construction of axially chiral sulfone-containing styrenes. *J. Am. Chem. Soc.* **140**, 7056–7060 (2018).
- Wu, S. et al. Urea group-directed organocatalytic asymmetric versatile dihalogenation of alkenes and alkynes. *Nat. Catal.* **4**, 692–702 (2021).
- Jin, L. et al. Atroposelective synthesis of axially chiral styrenes via an asymmetric C–H functionalization strategy. *Chem* **6**, 497–511 (2020).
- Ma, C. et al. Atroposelective access to oxindole-based axially chiral styrenes via the strategy of catalytic kinetic resolution. *J. Am. Chem. Soc.* **142**, 15686–15696 (2020).
- Qiu, S.-Q. et al. Asymmetric construction of an aryl-alkene axis by palladium-catalyzed Suzuki–Miyaura coupling reaction. *Angew. Chem. Int. Ed.* **61**, e202211211 (2022).
- Li, W. et al. Synthesis of axially chiral alkenylboronates through combined copper- and palladium-catalysed atroposelective aryl-boration of alkynes. *Nat. Synth.* **2**, 140–151 (2023).
- Ji, D. et al. Palladium-catalyzed asymmetric hydrophosphination of internal alkynes: Atroposelective access to phosphine-functionalized olefins. *Chem* **8**, 3346–3362 (2022).
- Wang, J. et al. Tandem iridium catalysis as a general strategy for atroposelective construction of axially chiral styrenes. *J. Am. Chem. Soc.* **143**, 10686–10694 (2021).

35. Zhang, X.-L. et al. Stepwise asymmetric allylic substitution-isomerization enabled mimetic synthesis of axially chiral B,N-heterocycles. *Angew. Chem. Int. Ed.* **61**, e202210456 (2022).
36. Sun, C. et al. Asymmetric allylic substitution-isomerization to axially chiral enamides via hydrogen-bonding assisted central-to-axial chirality transfer. *Chem. Sci.* **11**, 10119–10126 (2020).
37. Wu, Y.-X., Liu, Q., Zhang, Q., Ye, Z. & He, Y. Asymmetric allylic substitution-isomerization for accessing axially chiral vinylindoles by intramolecular $\pi\cdots\pi$ stacking interactions. *Cell Rep. Phys. Sci.* **3**, 101005 (2022).
38. Zou, J.-Y. et al. Asymmetric allylic substitution-isomerization for the modular synthesis of axially chiral *N*-vinylquinazolinones. *Angew. Chem. Int. Ed.* **62**, e202310320 (2023).
39. Strieth-Kalthoff, F., James, M. J., Teders, M., Pitzer, L. & Glorius, F. Energy transfer catalysis mediated by visible light: principles, applications, directions. *Chem. Soc. Rev.* **47**, 7190–7202 (2018).
40. Strieth-Kalthoff, F. & Glorius, F. Triplet energy transfer photocatalysis: unlocking the next level. *Chem* **6**, 1888–1903 (2020).
41. Großkopf, J., Kratz, T., Rigotti, T. & Bach, T. Enantioselective photochemical reactions enabled by triplet energy transfer. *Chem. Rev.* **122**, 1626–1653 (2022).
42. Wang, P.-Z., Xiao, W.-J. & Chen, J.-R. Light-empowered contra-thermodynamic stereochemical editing. *Nat. Rev. Chem.* **7**, 35–50 (2023).
43. Palai, A., Rai, P. & Maji, B. Rejuvenation of dearomative cycloaddition reactions via visible light energy transfer catalysis. *Chem. Sci.* **14**, 12004–12025 (2023).
44. Gloor, C. S., Dénès, F. & Renaud, P. Memory of chirality in reactions involving monoradicals. *Free Radic. Res.* **50**, S102–S111 (2016).
45. Schmalz, H.-G., de Koning, C. B., Bernicke, D., Siegel, S. & Pflerschinger, A. Memory of chirality in electron transfer mediated benzylic umpolung reactions of arene-Cr(CO)₃ complexes. *Angew. Chem. Int. Ed.* **38**, 1620–1623 (1999).
46. Lee, W., Koo, Y., Jung, H., Chang, S. & Hong, S. Energy-transfer-induced [3+2] cycloadditions of N–N pyridinium ylides. *Nat. Chem.* **15**, 1091–1099 (2023).
47. Becker, M. R., Wearing, E. R. & Schindler, C. S. Synthesis of azetidines via visible-light-mediated intermolecular [2+2] photocycloadditions. *Nat. Chem.* **12**, 898–905 (2020).
48. Zhang, X. et al. Extended single-electron transfer model and dynamically associated energy transfer event in a dual-functional catalyst system. *JACS Au* **3**, 1452–1463 (2023).
49. Yang, Y., Liu, L., Fang, W.-H., Shen, L. & Chen, X. Theoretical exploration of energy transfer and single electron transfer mechanisms to understand the generation of triplet nitrene and the C(sp³)-H amidation with photocatalysts. *JACS Au* **2**, 2596–2606 (2022).
50. Yang, Y. et al. Mechanistic understanding and reactivity analyses for the photochemistry of disubstituted tetrazoles. *J. Phys. Chem. A* **127**, 4115–4124 (2023).
51. Basilaia, M., Chen, M. H., Secka, J. & Gustafson, J. L. Atropisomerism in the pharmaceutically relevant realm. *Acc. Chem. Res.* **55**, 2904–2919 (2022).
52. Glunz, P. W. Recent encounters with atropisomerism in drug discovery. *Bioorg. Med. Chem. Lett.* **28**, 53–60 (2018).

Acknowledgements

We gratefully acknowledge the financial support from the National Natural Science Foundation of China (22201131 for Y.H.) and the Natural Science Foundation of Jiangsu Province (BK20220137 for Y.H.).

Author contributions

J.W. and J.G. contributed equally to this work. Y.H. designed and directed the project. J.W., J.-Y.Z., M.-J.Z., R.S., Z.Y., and P.-X.X. performed the experiments. J.G. performed the DFT calculations. Y.H. wrote the manuscript with the revisions of all authors.

Competing interests

The authors declare no competing interests.

Additional information

Supplementary information The online version contains supplementary material available at <https://doi.org/10.1038/s41467-024-47404-3>.

Correspondence and requests for materials should be addressed to Ying He.

Peer review information *Nature Communications* thanks the anonymous reviewer(s) for their contribution to the peer review of this work. A peer review file is available.

Reprints and permissions information is available at <http://www.nature.com/reprints>

Publisher's note Springer Nature remains neutral with regard to jurisdictional claims in published maps and institutional affiliations.

Open Access This article is licensed under a Creative Commons Attribution 4.0 International License, which permits use, sharing, adaptation, distribution and reproduction in any medium or format, as long as you give appropriate credit to the original author(s) and the source, provide a link to the Creative Commons licence, and indicate if changes were made. The images or other third party material in this article are included in the article's Creative Commons licence, unless indicated otherwise in a credit line to the material. If material is not included in the article's Creative Commons licence and your intended use is not permitted by statutory regulation or exceeds the permitted use, you will need to obtain permission directly from the copyright holder. To view a copy of this licence, visit <http://creativecommons.org/licenses/by/4.0/>.

© The Author(s) 2024